

Adaptive Multiuser Detection in Dispersive Channels with Array Observations

Steven D. Gray*

The MITRE Corp., Bedford, MA

James C. Preisig†

Woods Hole Oceanographic Inst., Dept. of Applied Ocean Physics and Engr., Woods Hole, MA

David Brady‡

Dept. of Electrical and Computer Engr. Northeastern University, Boston, MA

Abstract

We present a multiuser receiver which is capable of operating in time-variant channels with severe multipath. For each active user, the receiver consists of a multi-input, single-output filter followed by a single-user adaptive equalizer. The array processing filter is chosen to maximize an averaged performance metric which measures reduction in the interference from multiple asynchronous cochannel users and the reduction in intersymbol interference caused by time spreading of the transmitted signal. The single-user adaptive equalizer that follows the array processing filter eliminates the remaining intersymbol interference prior to hard symbol decisions. Receiver performance is demonstrated using data obtained from two acoustic channels where two cochannel users are transmitting in shallow-water at 18 and 30 nautical miles from the receiver array.

I. Introduction

We consider the problem of asynchronous multisource demodulation in a slowly time-varying channel using array observations. The model of a slowly time-varying medium is applicable to the simultaneous demodulation of multiple cochannel transmissions through an acoustic shallow-water or radio frequency cellular channel. Unlike nondispersive multiple-access channels, the acoustic and cellular channels are characterized by considerable multipath and difficulty in assigning a direction of arrival for each multipath component. As a result, the aggregate interference level for acoustic channels is greater than that for memoryless channels because of InterSymbol Interference (ISI).

Until recently, the major work in multiuser detection has been in the context of radio frequency digital com-

munications in which the channel is assumed known and the channel-induced ISI was neglected. Recent work has demonstrated the use of coherent combining of array observations and adaptive decision feedback equalization for single-user shallow-water systems [1]. The receiver parameters in this multi-input single output system were updated using Recursive Least Squares (RLS) estimation. In an additional application, an asynchronous receiver used observations at a single hydrophone to successfully demodulate two users in a shallow-water channel. Interference suppression was achieved by subtracting RLS estimates of the time-varying cochannel interference [2]. In both cases, system parameters were updated at the symbol rate.

The proposed receiver structure consists of a time-domain Array Processing Filter (APF) followed by an adaptive equalizer for each active user in the channel. Our use of array processing techniques is motivated by the desire to exploit the spatial diversity inherent in array observations to reduce the cochannel interference and the span of the ISI present at the input to the equalizer. The single-user equalizer assumes the burden of eliminating the remaining ISI in the signal. This division of labor between the array processor and the single-user equalizer is designed such that the APF exploits primarily the slowly-varying large scale multipath structure of the channel, subsequently called macro-multipath, and the equalizer adaptively tracks the rapid small-scale fluctuations in the channel, subsequently called micro-multipath. Therefore, the weights of the array processor can be updated less frequently than the weights of the equalizer. This will increase system performance and maintain modest receiver complexity.

II. Channel Model

Consider K asynchronous users transmitting to a single array of P sensors. The channel from each of the users to each of the sensors is a causal, slowly time-varying, Finite Impulse Response (FIR) channel. The

*Supported by the MITRE Corp. project number 91920.

†Supported in part by ARPA Grant MDA 972-91-J-1004 and in part by the Office of Naval Research by Grant N00014-91-J-1246.

‡Supported by ARPA Grant MDA972-93-1-0034.

i th data symbol for the k th user, $q_k[i]$, is modulated at the transmitter by a preassigned waveform, $s_k(t)$, which has compact support. Thus, for a message of Q symbols, the signal transmitted by the k th user can be expressed as

$$S_k(t) = \sum_{i=0}^{Q-1} q_k[i] s_k(t - iT - \tau_k). \quad (1)$$

Here, T is the reciprocal baud rate and τ_k is the relative time offset of the k th source. This signal from the k th user is received at the p th sensor after passing through a channel characterized by the input delay-spread function $g_{k,p}(t, \epsilon)$.¹ The signal from the k th user and received at the p th sensor, $u_{k,p}(t)$, is sampled with a period of T_s which is chosen so that $L = \frac{T}{T_s}$ is an integer.

Define the fractionally spaced input signal as

$$\check{q}_k[i] = \begin{cases} q_k[i/L] & i/L \text{ an integer} \\ 0 & i/L \text{ not an integer} \end{cases}$$

The sampled version of $u_{k,p}(t)$ is given by

$$u_{k,p}[n] = \sum_{i=0}^{LQ-1} \check{q}_k[i] g_{k,p}[n, n-i], \quad (2)$$

where

$$g_{k,p}[n, m] = \int_0^{NT_s} s_k(mT_s - \epsilon - \tau_k) g_{k,p}(nT_s, \epsilon) d\epsilon$$

is the effective discrete-time, input delay-spread function for the channel between the k th user and the p th sensor.

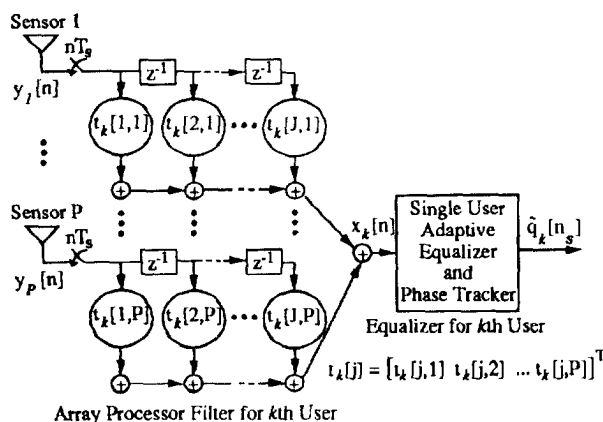


Figure 1: Proposed Receiver for the k th User

As shown in figure 1, the signal received at the p th sensor of the receiving array expressed in terms of (2)

¹The input delay-spread function $g_{k,p}(t, \epsilon)$ is the output of the channel at time t due to an impulse input to the channel at time $t - \epsilon$ [3]. For a time-invariant channel, the input delay-spread function $g_{k,p}(t, \epsilon)$ equals the time-invariant impulse response $h_{k,p}(\epsilon)$.

is given by $y_p[n] = \sum_{k=1}^K u_{k,p}[n] + \eta_p[n]$. $\eta_p[n]$ is a zero-mean process used to model sensor noise. However, knowledge of the second-order statistics for $\eta_p[n]$ are not required in the development that follows.

Given a causal FIR channel, it can be assumed that $g_{k,p}[n, m]$ equals zero for $m < 0$ and $m > (M - 1)$ for some integer M . Let the superscripts $*$ and h denote complex conjugate and Hermitian, respectively; and let boldface uppercase letters denote matrix quantities and boldface lowercase letters denote vector quantities. Then, letting

$$\mathbf{g}_k[n, m] = [g_{k,1}[n, m]^* \cdots g_{k,P}[n, m]^*]^h,$$

the discrete-time observations at the array of P sensors of the signal transmitted by the k th user can be expressed as

$$\mathbf{u}_k[n] = \sum_{m=n-M+1}^n \mathbf{g}_k[n, n-m] \check{q}_k[m]. \quad (3)$$

III. Receiver Structure

The proposed receiver for the k th user is shown in figure 1 and is comprised of the APF followed by a single user equalizer. Here, the symbol $\hat{q}_k[n_s]$ denotes an estimate of $q_k[n_s]$. The entire receiver for K users consists of K replicas of the structure shown in figure 1. The APF is a fractionally-spaced, multi-input, single-output linear filter. The filter weights are adapted several times per packet according to a performance metric which balances the maximization of the Signal-to-Interference Ratio (SIR) for the k th user with respect to the other users at the output of the APF (i.e., reduce the Multiple-Access Interference, MAI) and the reduction in the span of the ISI for the effective channel between the source for then k th user and the output of the APF.

Unlike the case for the single-user equalizer, the weights for the APF are updated at a rate that can be orders of magnitude slower than symbol rate. Therefore, the ability of the APF to suppress MAI and reduce ISI must be relatively robust with respect to channel fluctuations. This robustness is achieved by using estimates of the time-varying channel statistics when selecting the APF weights. The APF weights update interval is chosen so that the macro-multipath structure of the channel is relatively stable over the interval. Then, the APF can exploit the macro-multipath and remain insensitive to the rapid micro-multipath fluctuations.

A. Array Processor Filter

The input contribution to the APF input from the k th user is the sampled vector time-series, $\mathbf{u}_k[n]$. The samples are delayed, weighted, and then summed to form

the filter output. The output of the APF with weight vector \mathbf{t} due to the signal transmitted by the k th user is

$$x_{t,k}[n] = \sum_{j=0}^{J-1} t^h[j] \mathbf{u}_k[n-j], \quad (4)$$

where J is the number of temporal taps and $t[j]$ are the filter weights for the j th tap. While $t[j]$ are adapted, they are adapted at a packet rate and are temporarily assumed fixed. Combining (3) and (4) yields

$$x_{t,k}[n] = \sum_{m=0}^{M+J-2} h_{t,k}[n,m] \check{q}_k[n-m],$$

where

$$h_{t,k}[n,m] \approx \sum_{j=\max(0,m-M+1)}^{\min(J-1,m)} t^h[j] \mathbf{g}_k[n,m-j] \quad (5)$$

is the approximate effective discrete-time input delay-spread function for the channel between the fractionally spaced input signal for the k th user and the output of the APF with filter weights $t[j]$. The approximation is made assuming the channel, $\mathbf{g}_k[n,m]$ is slowly-time varying with respect to the time parameter n .

Using the symbol $\mathbf{0}$ to denote a $1 \times P$ vector of all zeros; and letting²

$$\mathbf{G}_k[n] = \begin{bmatrix} \mathbf{g}_k^h[0] & \mathbf{0} & \dots & \mathbf{0} \\ \mathbf{g}_k^h[1] & \mathbf{g}_k^h[0] & \ddots & \vdots \\ \vdots & \vdots & \ddots & \mathbf{0} \\ \mathbf{g}_k^h[J-1] & \dots & \dots & \mathbf{g}_k^h[0] \\ \vdots & \vdots & \vdots & \vdots \\ \mathbf{g}_k^h[M-1] & \dots & \dots & \mathbf{g}_k^h[M-J] \\ \mathbf{0} & \mathbf{g}_k^h[M-1] & \dots & \mathbf{g}_k^h[M-J+1] \\ \vdots & \ddots & \ddots & \vdots \\ \mathbf{0} & \dots & \mathbf{0} & \mathbf{g}_k^h[M-1] \end{bmatrix}$$

and

$$\mathbf{t} = \begin{bmatrix} t[0] \\ \vdots \\ t[J-1] \end{bmatrix},$$

(5) can be expressed in vector notation as

$$\mathbf{h}_{t,k}[n] = \begin{bmatrix} h_{t,k}[n,0] \\ \vdots \\ h_{t,k}[n,M+J-2] \end{bmatrix} = (\mathbf{G}_k[n] \mathbf{t})^*$$

²The dependence of the elements of the matrix $\mathbf{G}_k[n]$ on the absolute time parameter, n , has been dropped here for notational convenience. In addition, it has been assumed here that $J \leq M$. For the case of $M > J$, the form of $\mathbf{G}_k[n]$ will change slightly.

Given any $M+J-1$ element vector, \mathbf{v} , with non-negative real entries, the weighted energy in $\mathbf{h}_{t,k}[n]$ is given by

$$P_{t,k}[n, \mathbf{v}] = \mathbf{h}_{t,k}^h[n] \mathbf{D}(\mathbf{v}) \mathbf{h}_{t,k}[n] = \mathbf{t}^h \underbrace{\mathbf{G}_k^h[n] \mathbf{D}(\mathbf{v}) \mathbf{G}_k[n]}_{\mathbf{E}_k[n, \mathbf{v}]} \mathbf{t}.$$

Here, $\mathbf{D}(\mathbf{v})$ is a diagonal matrix with main diagonal elements taken from the vector \mathbf{v} . The weighted energy for all users is used in calculating the performance metric for the APF weights.

Assume that we are calculating the APF weights for the receiver demodulating user 1. Then, recall that tasks assigned to the APF are to reduce the interference caused by the signal from other users (MAI) and to reduce the support of the output response for user 1. In order to reduce the span of the ISI, the filtered input delay-spread function for user 1 ($h_{t,1}[n,m]$) is divided into three regions as a function of the delay index m . One region is the “shaped region” in which we want the energy in the response to be concentrated, one region is the “undesired region” in which we want the energy in the response to be suppressed, and the third region is an “unconstrained region” which is a buffer zone between the desired and undesired regions and is adjusted in a manner which allows the processor to concentrate or suppress the energy in the other regions. Let \mathbf{v}_{1d} and \mathbf{v}_{1u} be energy weight vectors with nonzero elements in only the elements corresponding to the desired and undesired regions of $h_{t,1}[n,m]$, respectively. In order to reduce the MAI for user 1, the energy in the filtered input delay-spread function for all interferers must be reduced. Therefore, a vector \mathbf{v}_k is defined for $k = 2 \dots K$ with nonzero elements over the entire span of the delay index of $h_{t,k}[n,m]$ and $P_{t,k}[n, \mathbf{v}_k]$.

For some exponential forgetting factor, $\rho \in (0, 1)$ and letting $\hat{\mathbf{G}}_k[n]$ denote the matrix $\mathbf{G}_k[n]$ based upon estimates of $\mathbf{g}_k[n,m]$ we define

$$\hat{\mathbf{E}}_k[n, \mathbf{v}] = \rho \hat{\mathbf{E}}_k[n-1, \mathbf{v}] + (1-\rho) \hat{\mathbf{G}}_k^h[n] \mathbf{D}(\mathbf{v}) \hat{\mathbf{G}}_k[n] \quad (6)$$

as a recursive estimate of $\mathbf{E}_k[n, \mathbf{v}]$. Now, we define a “signal-to-interference” cost function in terms of the weighted energies for each active user in the channel in terms of \mathbf{v}_{1u} , \mathbf{v}_{1d} , and \mathbf{v}_k where

$$\text{SIR}_1[\mathbf{t}, n] = \frac{\mathbf{t}^h \hat{\mathbf{E}}_1[n, \mathbf{v}_{1d}] \mathbf{t}}{\mathbf{t}^h (\sum_{k=2}^K \hat{\mathbf{E}}_k[n, \mathbf{v}_k] + \hat{\mathbf{E}}_1[n, \mathbf{v}_{1u}]) \mathbf{t}}. \quad (7)$$

For any n , the APF weights are given by

$$\mathbf{t}_{1,n} = \arg \max_{\mathbf{t} \in \mathcal{C}^{J,P}} \text{SIR}_1[\mathbf{t}, n]. \quad (8)$$

The $\mathbf{t}_{1,n}$ which maximizes this ratio is the generalized eigenvector of the matrix pencil $\hat{\mathbf{E}}_1[n, \mathbf{v}_{1d}] - \lambda (\sum_{k=2}^K \hat{\mathbf{E}}_k[n, \mathbf{v}_k] + \hat{\mathbf{E}}_1[n, \mathbf{v}_{1u}])$ corresponding to the

maximum eigenvalue λ_{\max} [4]. Since the computation of $\mathbf{t}_{1,n}$ requires the eigenvector corresponding to its maximum eigenvalue of the matrix pencil, the computationally efficient power method [5] may be used.

The final consideration in calculating $\mathbf{t}_{1,n}$ is the phase response of the APF. In calculating $\mathbf{t}_{1,n}$, no restrictions were placed on the phase introduced by the APF. However, when switching from one set of filter weights \mathbf{t}_{1,n_1} to a new set of filter weights \mathbf{t}_{1,n_2} , a phase discontinuity may be introduced. Abrupt changes in the phase degrades demodulator performance by disturbing the weights in the adaptive equalizer. However, APF induced phase discontinuities are easily overcome by calculating the step response of the APF and scaling the array weights such that the steady state phase response is zero. The response of the APF, with weights $\mathbf{t}_{1,n}$, to a unit step input at all sensors is given by $R_1 e^{j\psi_1} = \sum_{j=1}^J \sum_{p=1}^P t_{1,n}[j,p]$ where R_1 is the steady-state magnitude response and ψ_1 is the steady state phase response. Thus, the desired array weight vector with zero phase response that satisfies (8) is $\mathbf{t}_{1,n} e^{-j\psi_1}$.

B. Adaptive Equalization

The equalizer shown in figure 2 consists of a feedforward section, feedback section and a tracking loop with phase estimates of the equalizer input. The equalizer input, $\mathbf{x}_k[n] = \sum_{i=1}^K x_{i,k}[n] + \tilde{\eta}[n]$, is the output of the APF for weight vector $\mathbf{t}_{k,n}$ from all active users in the channel. Here, $\tilde{\eta}[n]$ is the APF output noise process.

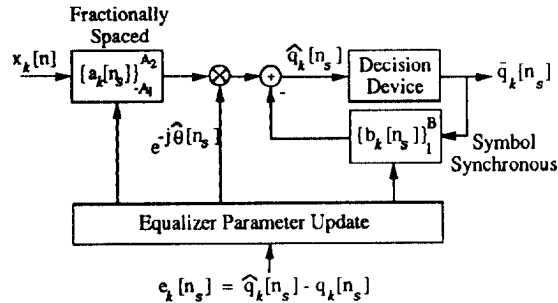


Figure 2: Adaptive Single User Decision Feedback Equalizer

The weight vector for the fractionally spaced feedforward section of the equalizer, $\mathbf{a}_k[n_s]$ and the weight vector for the symbol-rate feedback section of the equalizer, $\mathbf{b}_k[n_s]$ are updated once per symbol. We use n_s to denote the symbol index where $n_s = \text{int}[n/L]$. The total number of feedforward taps is $A_1 + A_2 + 1$ and the total number of feedback taps is B . The output of the equalizer's feedforward section is multiplied by a complex exponential containing $\hat{\theta}[n_s]$, an estimate of the Doppler rate for the k th user. The decision device in Figure 2 is determined by assuming that all ISI and MAI has been

removed from $\hat{q}_k[n_s]$ and only additive white Gaussian noise now corrupts $q_k[n_s]$. In addition, RLS estimation is used to update the equalizer taps; mathematical details can be found in [1].

IV. Experimental Results

To demonstrate the performance of the proposed receiver, we present results from data transmitted through two shallow water channels off the coast of New England. Two sources transmitted narrowband Quadrature Phase Shift Keyed (QPSK) packets at a rate of 333 symbols per second with a common carrier frequency and a range of 18 and 30 nautical miles from the receiver array. The QPSK symbols sent by both users were shaped using raised cosine pulses where each user transmitted a total of 2047 symbols. Because the data collected for the two users was at different times, a multi-user collision is emulated by adding the two data sets. In addition, the SIR at the hydrophone array is set for our experiment to 0 dB by normalizing the 18 and 30 nautical mile data before the two records are added together. Both channels had approximately 30 symbols of memory.

Two cases are compared. The first corresponds to a hypothetical single sensor, single user equalizer that does not suppress cochannel interference prior to equalization and the second corresponds to an APF followed by a single user equalizer. In both cases, the number of taps in the adaptive single-user equalizer is selected such that the number of errors at the equalizer output is minimized. The APF in the second case combines six sensors of observations with a tap delay length of 10 symbols. The sampling rate of the input signal and amount of fractionally spacing in the APF is four times the baud rate. The fractionally spacing in the feedforward section of the equalizer was reduced to two samples per symbol to reduce equalizer complexity.

The first case described in the preceding paragraph corresponds to a single hydrophone collecting the samples for two users' transmissions. The decision feedback equalizer shown in figure 2 is operated in "training"³ mode during the first 1047 symbols in the packet and "decision feedback" mode over the last 1000 symbols in the packet for the 30 nautical mile user. The fractionally spaced feedforward section of the equalizer had 120 taps and the symbol synchronous feedback section had 70 taps. Our method for evaluating performance is to assume the equalizer converges over the first half of the packet and to plot $\hat{q}_k[n_s]$, the equalizer output prior to hard decisions, over the last half of the packet. However, figure 3 illustrates that in this case, the equalizer is unable to achieve convergence to a meaningful solution and

³Training mode means that the error, $e_k[n_s]$, contains the correct symbol $q_k[n_s]$ rather than $\hat{q}[n_s]$ as in decision feedback mode.

reliably demodulate the 30 nautical mile user when the 18 nautical mile user is of equal strength. A total of 235 errors occurred in demodulating the last 1000 symbols of the 30 nautical mile user's data packet.

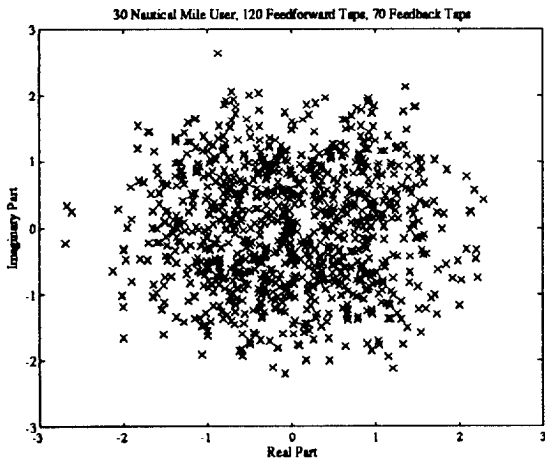


Figure 3: Equalizer Output, $\hat{q}_k[n_s]$, for the 30 Nautical Mile User Prior to Hard Decisions with no APF

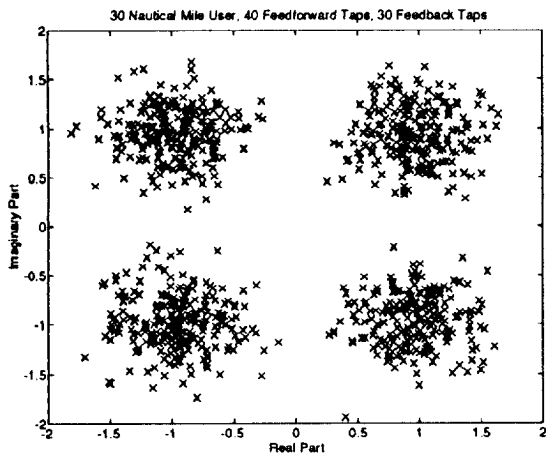


Figure 4: Equalizer Output, $\hat{q}_k[n_s]$, for the 30 Nautical Mile User Prior to Hard Decisions with APF

The second case presented corresponds to the same communication channel as the first case, except now the APF suppresses the 18 nautical mile transmission prior to adaptive equalization. Least squares estimates of the delay spread matrices $\mathbf{G}_1[n]$ and $\mathbf{G}_2[n]$, are used in the estimators $\hat{\mathbf{E}}_1[n, \mathbf{v}_{1d}]$, $\hat{\mathbf{E}}_2[n, \mathbf{v}_2]$ and $\hat{\mathbf{E}}_1[n, \mathbf{v}_{1u}]$ for determining $\mathbf{t}_{1,n}$. The APF parameters were selected such that the ISI for the 30 nautical mile user at the equalizer input would have a support of approximately 10 symbols. Six sensors with a depth equivalent to 10 symbol periods were combined in the suppression of the 18

nautical mile user to a level 13.8 dB below the 30 nautical mile user. In addition, the weights in the APF were fixed over the whole packet.

Unlike the case shown in figure 3, the adaptive equalizer that follows the APF achieved convergence to a meaningful solution. The adaptive equalizer's feedforward section had 40 taps and the feedback section had 30 taps. Figure 4 is a plot of $\hat{q}_k[n_s]$ over the last half of the packet for the same user we previously attempted to demodulate with only an adaptive equalizer. No errors occurred in the demodulation of the last 1000 symbols.

V. Conclusions

The APF proposed in this paper offers an effective and robust method for reducing the cochannel interference caused by multiple users communicating in a multiple access channel. The reduction in cochannel interference is achieved by exploiting the spatial and temporal differences in the signals received across an array. The APF is implemented adaptively to track changes in the channel statistics and to maximize a performance criterion that takes into account both cochannel and intersymbol interference. The APF adaptation is designed to allow the processor to exploit the slowly time-varying macro-multipath structure of the channel without having to track the rapidly varying micro-multipath characteristics. As a result, a typical APF update rate is much greater than a symbol duration. A symbol-adaptive single-user equalizer then tracks and compensates for the micro-multipath characteristics of the channel.

References

- [1] Stojanovic, M., "Coherent Digital Communications for Rapidly Fading Channels with Applications to Underwater Acoustics," Ph.D. Thesis, Northeastern Univ., Boston MA, Sept. 1993.
- [2] Zvonar, Z., D. Brady, "Adaptive Multiuser Receiver for CDMA Fading Channels with Severe ISI," The Conf. on Information Sciences and Systems, The Johns Hopkins Univ., Baltimore, MD, March, 1993.
- [3] Bello, Philip A., "Characterization of Randomly Time-Variant Linear Channels," *IEEE Trans. on Communications Systems*, CS-11, December 1963, pp. 360-393.
- [4] Golub, G., C. Van Loan, *Matrix Computations*, The Johns Hopkins University Press, Baltimore, MD, p. 251, 1983.
- [5] Kozłowski, W., "The power method for the generalized eigenvalue problem," *Roczniki Polskiego Towarzystwa Matematycznego, Seria III, Matematyka Stosowana, Applied Mathematics*, vol. 35, 1992, pp. 21-32.